Correlation between metal-insulator transition characteristics and electronic structure changes in vanadium oxide thin films

Dmitry Ruzmetov,[1] Sanjaya D. Senanayake,[2] Venkatesh Narayanamurti,[1] and Shriram Ramanathan[1]
[1]*Harvard School of Engineering and Applied Sciences, Harvard University, Cambridge, Massachusetts 02138, USA*
[2]*Chemical Sciences Division, Oak Ridge National Laboratory, Oak Ridge, Tennessee 37831, USA*
(Received 4 December 2007; revised manuscript received 14 April 2008; published 29 May 2008)

We correlate *electron transport data* directly with energy band structure measurements in vanadium oxide thin films with varying V-O stoichiometry across the VO_2 metal-insulator transition. A set of vanadium oxide thin films were prepared by reactive dc sputtering from a V target at various oxygen partial pressures (O_2 p.p.). Metal-insulator transition (MIT) characteristic to VO_2 can be seen from the temperature dependence of electrical resistance of the films sputtered at optimal O_2 p.p. Lower and higher O_2 p.p. result in disappearance of the MIT. The results of the near edge x-ray absorption fine structure spectroscopy of the O *K* edge in identical VO films are presented. Redistribution of the spectral weight from σ^* to π^* bands is found in the vanadium oxide films exhibiting stronger VO_2 MIT. This is taken as evidence of the strengthening of the metal-metal ion interaction with respect to the metal-ligand and indirect V-O-V interaction in vanadium oxide films featuring sharp MIT. We also observe a clear correlation between MIT and the width and area of the lower π^* band, which is likely to be due to the emergence of the $d_{||}$ band overlapping with π^*. The strengthening of this $d_{||}$ band near the Fermi level only in the vanadium oxide compounds displaying the MIT points out the importance of the role of the $d_{||}$ band and electron correlations in the phase transition.

DOI: 10.1103/PhysRevB.77.195442 PACS number(s): 78.70.Dm, 71.30.+h, 71.27.+a, 72.80.Ga

I. INTRODUCTION

Vanadium dioxide exhibits a metal-insulator transition (MIT) close to room temperature (T_{MIT}=67 °C in bulk crystals).[1] Sharp changes in optical parameters of VO_2 near T_{MIT} are present as well.[2] These switching properties along with recent reports that the transition can be induced by an electric field[3,4] excite interest in the material from fundamental science and electronic application perspectives. The high temperature (above T_{MIT}) metallic phase has a tetragonal lattice[5] and the low-*T* semiconducting phase has a monoclinic lattice.[6] Whether this lattice transformation or electron correlations are primarily responsible for the MIT are still the subject of intense research.[7–10] In this view, the information on which elements of the band structure of vanadium oxides are characteristic to samples exhibiting sharp VO_2 MIT is important for understanding the physical origin of the MIT and utilizing the effect in advanced devices. Future applications of VO_2 in electronics may involve thin films, whereas a number of studies so far have been done on VO_2 single crystals. Depending on the stoichiometric purity of the compound and its crystal structure, the MIT parameters significantly vary. This effect is especially pronounced in thin films due to their granular structure, dependence on the choice of substrate, and nonstoichiometry determined by synthesis conditions.

In this paper, we address an issue encountered in thin VO_2 films, which is the variation of electrical parameters in a set of VO_x thin films synthesized under similar conditions. We investigate the band structure near the Fermi level of these films using x-ray absorption spectroscopy (XAS). The distinction of this study is that we scrutinize the band structure in the VO_2 compounds of very close stoichiometry and composition whose metal-insulator transition parameters strongly vary at the same time. Our study finds a clear correspondence between the MIT strength and specific energy band parameters extracted from the XAS spectra. These results are important since they directly emphasize the features of the band structure responsible for MIT, as compared to the studies on various vanadium oxide compounds, such as VO_2, V_2O_3, V_2O_5, and other transition metal oxides whose large differences in crystal lattice and electronic configuration of the cation may cause band structure changes with little connection to the MIT specific to VO_2.

X-ray absorption spectroscopy has proven to be a powerful tool to study the unoccupied density of states (UDOS) of VO_2 near the Fermi level. Oxygen *K*-edge absorption spectra in this paper correspond to electron excitations from O 1*s* to unoccupied O 2*p* orbitals. The latter are hybridized with V 3*d* orbitals and lie close to the Fermi level. The dipole selection rules require transitions with orbital momentum change $\Delta l = \pm 1$ so that O *K*-edge XAS intensity reflects the *p*-projected UDOS of the valence levels. Differences in UDOS were measured by XAS [specifically, near edge x-ray absorption fine structure (NEXAFS)] in metallic and semiconducting phases of VO_2 and in thin films of different morphology.[11,12] The analysis of the measured XAS data in VO_2 and their comparison to density of states (DOS) calculations are determining factors for selecting viable theoretical models describing the MIT and understanding the origin of the phase transition.[13–15]

II. EXPERIMENTAL DETAILS

Vanadium oxide thin films were reactively sputtered in $Ar(100\%-x)+O_2(x)$, where x=6.8%, 7.8%, 8.8%, 9.8%, and 10.8%, environment at 10 mTorr from a *V* target. The substrate was kept at 550 °C during the deposition. The amount of Ar and O_2 in the sputtering chamber was carefully controlled by mass flow controllers. The VO_2 film thickness was

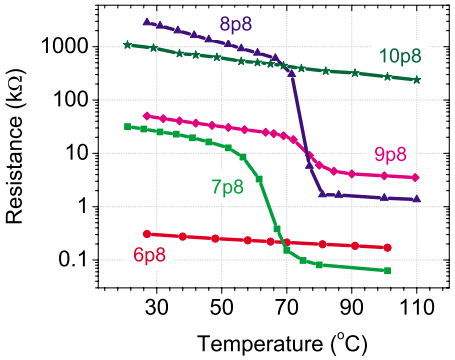

FIG. 1. (Color online) Temperature dependence of the sample resistance. Optimally synthesized samples 7*p*8 and 8*p*8 show MIT.

fixed at 100 nm. The electrical resistance measurements were done using an environmental probe station at atmospheric pressure with two probes contacting the surface of a VO_2 film on Si/SiO_2 substrate. Linear *I*-*V* curves were measured with voltages of up to 0.02 V to calculate the resistance while the sample stage temperature was stabilized at a preset value. The temperature stabilization was performed by monotonous rather than an oscillatory approach to avoid errors due to the thermal hysteresis. X-ray absorption spectroscopy was done at the beamline U12a of the National Synchrotron Light Source (Brookhaven National Laboratory). The details of the measurements and photon calibration procedure are described elsewhere.[11]

III. RESULTS AND DISCUSSION

The results of the electrical resistance measurements on five characteristic samples are shown in Fig. 1. The samples were prepared at varying argon-oxygen ratios in the chamber during sputtering while all other deposition parameters were kept identical. The electrical parameters of the MIT in the samples are summarized in Table I. In order to extract the transition temperatures (T_{MIT}) and widths (ΔT), the derivatives $d(\log_{10} R)/dT$ were taken from the data in Fig. 1. The resulting curves had clear minima and could be well fitted with Gaussians (see examples of the fittings in Ref. 2). The center and the width of the fitted Gaussian were taken as

TABLE I. Metal-insulator transition parameters extracted from Fig. 1 (vanadium oxide thin films of varying V-O ratio near VO_2 stoichiometry). ID—sample ID, O_2—oxygen partial pressure during sputtering, T_{MIT}—MIT temperature, ΔT—MIT width, R_{MIT}—film resistance at T_{MIT} or at 72 °C for samples 6*p*8 and 10*p*8, and MIT strength—ratio of resistances at temperatures $T_{MIT} - / + \Delta T$.

ID	O_2 (%)	T_{MIT} (°C)	ΔT (°C)	R_{MIT} ($k\Omega$)	MIT strength
6*p*8	6.8		0	0.21	1
7*p*8	7.8	65	10	1.08	104
8*p*8	8.8	75	7	33.0	320
9*p*8	9.8	76	9	10.1	5
10*p*8	10.8		0	430	1

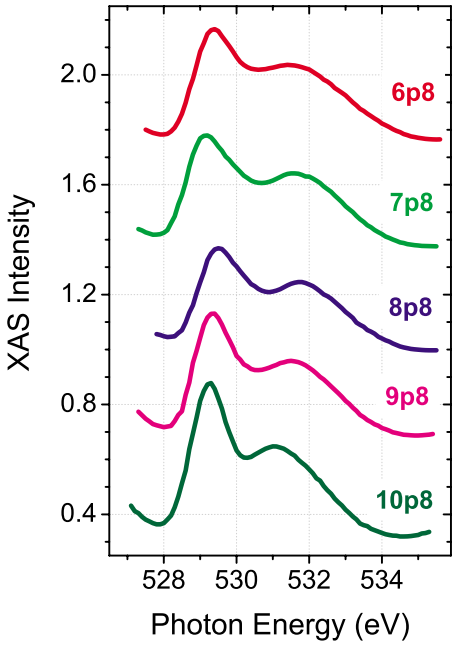

FIG. 2. (Color online) Measured XAS spectra of the oxygen *K* edge for the samples listed in Table I. The intensity is normalized to the maximum at V *L* edge (not shown) at approximately 518 eV measured in the same run with the O *K* edge. The intensity is translated up for clarity with an increment of 0.35 for graphs above 10*p*8.

T_{MIT} and ΔT. The MIT strength was defined as the resistance ratio $R(T_{MIT}-\Delta T)/R(T_{MIT}+\Delta T)$.

The data in Fig. 1 and Table I show how the MIT is sensitive to V-O stoichiometry. A 4% increase in oxygen content from 6.8% to 10.8% would completely miss the transition. With gradual increase in oxygen content, the resistance curves in Fig. 1 transform from almost metallic behavior (low resistance but semiconducting temperature dependence) at 6.8% to characteristic MIT curves at 7.8% and 8.8% and to a featureless high resistance line again at 10.8%. The synthesized films are polycrystalline and are expected to consist of predominantly VO_2 phase with the presence of small amounts of other vanadium oxide phases (e.g., such as V_2O_3 in oxygen deficient and V_2O_5 in O_2 excessive compounds). The defects and minor nonstoichiometric inclusions account for the smeared sharpness of the VO_2 metal-insulator transition in *R* vs *T* curves in Fig. 1. For example, oxygen deficient sample 7*p*8 has overall low resistance as compared to two other MIT samples, 8*p*8 and 9*p*8. Apparently, there are some metallic grains in the sample 7*p*8 which do not undergo the phase transition and lower the total resistance. Similarly, the oxygen-excess sample 9*p*8 is likely to have some higher valence vanadium oxide phase inclusions that remain semiconducting in the whole temperature range increasing the overall resistance.

X-ray absorption spectroscopy was done on identical VO_2 films on Si substrates, as described in Table I and Fig. 1. The XAS measurement results of the oxygen *K* edge at room temperature are shown in Fig. 2. The XAS intensity is normalized to the maximum of the nearby V *L* edge (not shown) at around 518 eV measured in the same run with O *K* edge,

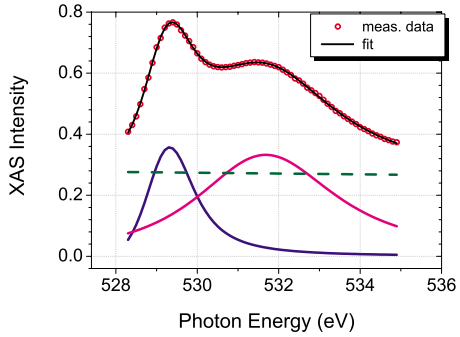

FIG. 3. (Color online) An illustration of the fitting procedure. The measured XAS data for sample 6*p*8 (circles) are fitted using a FITXPS software package (Ref. 16). The calculated fit (solid line through the data) is an algebraic sum of the three components in the lower part of the graph.

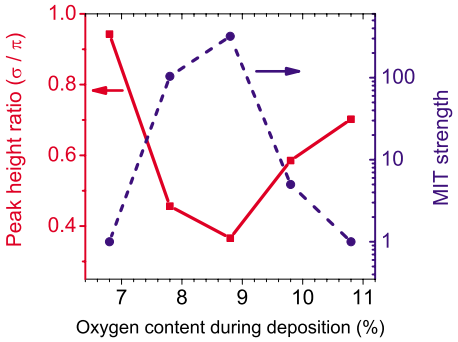

FIG. 4. (Color online) Relative heights of σ^* and π^* peaks extracted from the fitting to the XAS spectra in Fig. 2 in comparison to the VO_2 MIT strength (i.e., ratio of resistances at temperatures $T_{MIT}-/+\Delta T$).

so that a comparison of the absolute intensities between the graphs in Fig. 2 can be made. The resolution of the measured spectra is 0.1 eV (within one scan), while the absolute value of the photon energy may fluctuate within 0.4 eV from one scan to another. Each spectrum in Fig. 2 consists of two peaks corresponding to π^* and σ^* bands above the Fermi level.[11,12] To extract quantitative information from the spectra, each graph in Fig. 2 was fitted with the algebraic sum of π^*, σ^* peak, and linear background. An example of a fit is shown in Fig. 3. The line shape of each peak is a numerical convolution of an analytical Doniach–Sunjic[17] line shape with a Gaussian. The asymmetry of the peak was taken into account with the Doniach–Sunjic[17] parameter α, where $\alpha=0$ corresponds to a symmetric Lorentzian line shape. The Gaussian represents the broadening due to the experimental instrument function and possible broadening of the core-electron line shape due to thermal vibrations and static disorder.[18] Figure 3 demonstrates the importance of multicomponent fitting to the spectra in order to extract quantitative information about individual peaks.

Fitting results are presented in Table II. The goodness of fit is characterized with the parameter ε which is an average deviation of the fit from the measured spectrum relative to the spectrum amplitude,

$$\varepsilon = \frac{1}{N}\sum_{i=1}^{N}\frac{|E_i - f_i|}{E_{\max} - E_{\min}},$$

where N is the number of data points in the fitting range (varied from 58 to 67), E_i is the measured XAS intensity at a data point i, f_i is the calculated fit value, $E_{\max}=\max(E_i)$, and $E_{\min}=\min(E_i)$. As one can see from Table II, the fit deviation is less than 1% of the spectrum amplitude for all samples.

It can be seen from the fitting results that while π^* peak height fluctuates near 0.42 with no obvious difference between the VO_2 films with and without MIT, the σ^* peak height is proportionally lower in the samples with larger MIT strength. On the other hand, there is a clear tendency that the width of the π^* peak is larger in samples displaying strong MIT. These features result in π^* (σ^*) peak area being larger (smaller) in the samples with strong MIT. The same behavior is seen in the ratio of peak intensities. To illustrate this point, we plot in Fig. 4 the ratio of σ^* and π^* peak heights in comparison to the MIT strength. We see a clear redistribution of the spectral weight from σ^* toward π^* peak in samples with strong MIT. The σ^*/π^* peak area ratio graph (not shown) exhibits the same tendency. To summarize the results in Table II, the ratios of the σ^* and π^* peak parameters extracted from XAS data and the absolute values of the peak areas are strongly correlated with the MIT strength of the VO_2 films. However, the absolute values of peak heights and widths are not necessarily correlated with the MIT properties, which means that there is a transformation of the shape of the peaks seen in the XAS spectra in the samples with and without MIT. It is worthwhile to note that the large values of the linewidths of samples 7*p*8 and 8*p*8 extracted from the fitting are the result of two contributions: increased widths of the intrinsic Lorentzian and Gaussian curves and increased skew character of the XAS peaks. The latter can be seen in Fig. 2 and is taken into account by the Doniach–Sunjic[17] asymmetry parameter. The raised upper energy side of the peak increases its full width at half maximum (FWHM).

To infer qualitative information about the mechanism responsible for the change in relative XAS intensities in Fig. 4, it is useful to recall the band structure of VO_2 near the Fermi level based on the molecular-orbital and crystal field model

TABLE II. Oxygen *K*-edge XAS results for vanadium oxide films near the VO_2 stoichiometry and with various MIT strength. The data are obtained from the fitting to the measured spectra using the fitting procedure illustrated in the Fig. 3 and described in the text. $\Delta_{\pi\sigma}$—the separation between π^* and σ^* peaks. ε characterizes the fit goodness; see text.

Sample ID	Peak height		$\Delta_{\pi\sigma}$ (eV)	FWHM (eV)		Peak area		ε
	π^*	σ^*		π^*	σ^*	π^*	σ^*	$\times 10^{-3}$
6*p*8	0.35	0.33	2.4	1.4	4.1	0.54	1.81	3.6
7*p*8	0.46	0.21	2.9	3	2.9	1.43	0.78	6.1
8*p*8	0.41	0.15	2.4	3.9	4.9	1.23	0.62	6.5
9*p*8	0.41	0.24	2.4	1.7	3.2	0.87	0.93	5.3
10*p*8	0.47	0.33	2.1	1.2	3.2	0.73	1.49	7.1

employed by Goodenough.[19] The electronic configuration of the V ion in VO_2 is $3d^1$, so that V $3d$ levels need to be considered. Vanadium $3d$ states are split by the octahedral crystal field into upper e_g and lower t_{2g} levels. The empty V e_g orbitals form an antibonding σ^* band that gives rise to the upper absorption peak in Fig. 3.[12,15] The t_{2g} levels are located near the Fermi level and are further split by the total crystal field into a π^* doublet and a $d_\parallel$ level. The low temperature ($T < T_{MIT}$) monoclinic phase of insulating VO_2 is formed from the high-T tetragonal (rutile) phase by pairing and tilting of the V ions along the rutile c axis. Consequently, in the insulating phase, the $d_\parallel$ band is split into filled bonding and empty antibonding bands and π^* is pushed up from the Fermi level opening the band gap. Then, the lower band seen in Fig. 2 consists of π^* and antibonding $d_\parallel$ bands which sometimes can be separately resolved in polarization sensitive XAS of the O K edge in single crystal VO_2.[12,15] The $d_\parallel$ orbitals are directed along the rutile c axis, toward the next nearest neighbor V ions and are weakly hybridized with the π^* orbitals, so that the $d_\parallel$ band is characteristic of direct V-V interactions. The symmetry of the π and π^* orbitals is that most of the electron density is shifted away from the V-O bond direction and the orbitals point in between the ligands (O ions). On the other hand, bonding and antibonding σ orbitals have rotational symmetry around the V-O internuclear line and most of their electron density is close to the V-O line, so that σ orbitals point toward the ligands. The observed redistribution of the spectral weight in Fig. 4 from the upper to lower band in MIT samples indicates strengthening of the π^* and/or $d_\parallel$ bands with respect to the σ^* band. Since in both orbitals responsible for the π^* and $d_\parallel$ bands the electron density is shifted away from the V-O bond line as compared to the σ^* orbitals, the noted redistribution may be connected to the decrease in the direct V-O interaction and the increase in the V-V interactions. Assuming that the strengths (i.e., DOS) in conjugate antibonding and bonding bands are connected, one can judge that there is strengthening of the metal bonding and weakening of the direct metal-ligand interactions as the vanadium oxide compound approaches stoichiometric phase of pure VO_2 with a strong MIT.

Strongly differing σ^*/π^* relative peak intensities have been reported in VO_2 single crystals and powders.[12,15,20,21] Our results are closer to the x-ray absorption data on VO_2 powders which revealed the dominance of the first (π^*) peak in the raw spectra.[21] The reported spectra of the O K edge in single crystals depend on the polarization orientation of the x rays with respect to the crystal axes. When the x-ray photon polarization has the electric field vector parallel to the rutile crystal c axis ($E \| c$), the lower band peak in Fig. 2 splits into two peaks assigned as π^* and $d_\parallel$.[12,15] In this case, the intensity of the upper band σ^* may be comparable or higher than those of π^* and $d_\parallel$ peaks. For the other polarization orientation ($E \perp c$), the $d_\parallel$ peak is not resolved (suppressed due to the linear orbital orientation along the c axis) and the π^* peak dominates over σ^*. Then, the increased width and area of the π^* peak in our samples with strong MIT (see Table II) may be a manifestation of the emergence of the $d_\parallel$ band in these samples. The peak is not completely resolved because our spectra are the result of averaging of all polarization orientations in the polycrystalline films.

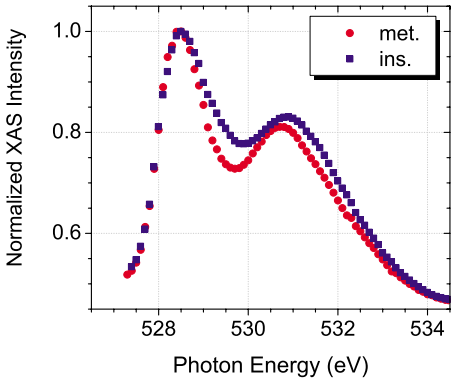

FIG. 5. (Color online) NEXAFS spectra for the VO_2 sample identical to $8p8$ showing the O K edge in the insulating (T=55 °C) and metallic (T=80 °C) phases of VO_2. The decrease in the linewidths upon MIT is visible.

Theoretical models describing the MIT within the Mott–Hubbard picture[9,22] have recently received more support.[10] In this picture, the transition is attributed to strong electron-electron correlations mostly in the $d_\parallel$ band. Also, a recent model suggested by Biermann *et al.*[23] based on cluster dynamical mean field theory (CDMFT) calculation shows that both correlation (Mott) and band (Peierls) effects are present. The model is well supported by x-ray photoemission spectra (XPS) of the valence bands of VO_2.[13] This CDMFT calculation finds a large redistribution of the electronic occupancies in favor of the $d_\parallel$ orbital. The importance of electron correlations is generally acknowledged when one needs to account for the transport properties of VO_2 and the $d_\parallel$ band is considered to play a crucial role in the MIT. Our results obtained from a set of vanadium oxide compounds with varying anion nonstoichiometry show that the appearance of this $d_\parallel$ band near the Fermi level in the spectra is directly related to the presence of the metal-insulator transition.

Temperature dependent NEXAFS measurements were performed on a VO_2 thin film sample synthesized under identical conditions as the sample $8p8$ in Table I. The O K-edge spectra across the metal-insulator transition are shown in Fig. 5. The spectra are normalized to the maximum of intensity at the O π^* peak and shifted horizontally within 0.1 eV (the resolution of the measurement) to coincide at the maximum of intensity, so that a visual comparison of linewidths was possible. One can see that the linewidths are reduced upon the phase transition to the metallic state. Specifically, the widths of π^* and σ^* peaks go down to 2.2 and 3.7 eV, respectively. The T=55 °C spectrum overlaps closely with the $8p8$ room temperature spectrum in Fig. 2 (neglecting the change in the slope of the background due to different incident photon intensities). The dependence of O K edge across the phase transition was studied in detail in our previous paper,[11] where we demonstrated that the decrease in linewidths occurred only upon crossing the T_{MIT} and the spectra remained unchanged while the temperature was varied either below or above T_{MIT}. The manifestation of the MIT in the XAS spectra in Fig. 5 is an important proof that the presented XAS study characterizes MIT-active VO_2

material of the films rather than a superficial layer on top of the film consisting of an overoxidized vanadium oxide.

In summary, the energy band structure of the valence levels of the vanadium oxide thin films with near VO_2 stoichiometry has been studied using x-ray absorption spectroscopy and electrical transport measurements of the metal-insulator transition were also performed on identical samples. We observe a clear correlation between the strength of the MIT and the relative spectral weight of the σ^* and π^* bands in the XAS O *K* edge. The increased intensity of the π^* peak with respect to the σ^* peak in samples with strong MIT can be interpreted as the weakening of the metal-ligand bonds and increasing of the role of the direct metal-metal ionic interactions. The spectra from samples with strong MIT show increased width and area of the lower band peak π^* which may be a manifestation of the emergence of the $d_{\|}$ peak. The increased spectral weight of this band is a unique property of samples with the metal-insulator transition. The presented results are of potential relevance to understanding the physical origin of the phase transition, developing comprehensive theoretical models of the MIT, and synthesis of VO_2 thin films with improved MIT parameters.

ACKNOWLEDGMENTS

This work was primarily supported by the NSF-SIA Supplement to the Nanoscale Science and Engineering Initiative under NSF Award No. PHY-0601184. S.D.S. would like to acknowledge the research sponsored by the Division of Chemical Sciences, Geosciences, and Biosciences, Office of Basic Energy Sciences, U.S. Department of Energy, under Contract No. DE-AC05-00OR22725, with Oak Ridge National Laboratory, managed and operated by UT-Battelle, LLC. The use of the National Synchrotron Light Source, Brookhaven National Laboratory, was supported by the U.S. Department of Energy, Office of Science, Office of Basic Energy Sciences, under Contract No. DE-AC02-98CH10886.

[1] F. J. Morin, Phys. Rev. Lett. **3**, 34 (1959).
[2] D. Ruzmetov, K. T. Zawilski, V. Narayanamurti, and S. Ramanathan, J. Appl. Phys. **102**, 113715 (2007).
[3] P. P. Boriskov, A. A. Velichko, A. L. Pergament, G. B. Stefanovich, and D. G. Stefanovich, Tech. Phys. Lett. **28**, 406 (2002).
[4] H.-T. Kim, B.-G. Chae, D.-H. Youn, G. Kim, K.-Y. Kang, S.-J. Lee, K. Kim, and Y.-S. Lim, Appl. Phys. Lett. **86**, 242101 (2005).
[5] D. B. McWhan, M. Marezio, J. P. Remeika, and P. D. Dernier, Phys. Rev. B **10**, 490 (1974).
[6] J. M. Longo and P. Kierkegaard, Acta Chem. Scand. (1947-1973) **24**, 420 (1970).
[7] R. M. Wentzcovitch, W. W. Schulz, and P. B. Allen, Phys. Rev. Lett. **72**, 3389 (1994).
[8] A. Cavalleri, T. Dekorsy, H. H. W. Chong, J. C. Kieffer, and R. W. Schoenlein, Phys. Rev. B **70**, 161102(R) (2004).
[9] M. S. Laad, L. Craco, and E. Muller-Hartmann, Phys. Rev. B **73**, 195120 (2006).
[10] H.-T. Kim, Y. W. Lee, B.-J. Kim, B.-G. Chae, S. J. Yun, K.-Y. Kang, K.-J. Han, K.-J. Yee, and Y.-S. Lim, Phys. Rev. Lett. **97**, 266401 (2006).
[11] D. Ruzmetov, S. D. Senanayake, and S. Ramanathan, Phys. Rev. B **75**, 195102 (2007).
[12] M. Abbate, F. M. F. de Groot, J. C. Fuggle, Y. J. Ma, C. T. Chen, F. Sette, A. Fujimori, Y. Ueda, and K. Kosuge, Phys. Rev. B **43**, 7263 (1991).
[13] M. Haverkort *et al.*, Phys. Rev. Lett. **95**, 196404 (2005).
[14] A. Cavalleri, M. Rini, H. H. W. Chong, S. Fourmaux, T. E. Glover, P. A. Heimann, J. C. Kieffer, and R. W. Schoenlein, Phys. Rev. Lett. **95**, 067405 (2005).
[15] T. C. Koethe *et al.*, Phys. Rev. Lett. **97**, 116402 (2006).
[16] D. Adams, FITXPS Version 2.12 (http://www.sljus.lu.se/download.html) software from, University of Aarhus (Denmark), was used to analyze the XPS and XAS spectra. The XAS spectra were inverted in photon energy before fitting with the program.
[17] S. Doniach and M. Sunjic, J. Phys. C **3**, 285 (1970).
[18] J. Stohr, *NEXAFS Spectroscopy* (Springer-Verlag, Berlin, Heidelberg 1992), Chap. 7.
[19] J. B. Goodenough, J. Solid State Chem. **3**, 490 (1971).
[20] E. Goering, O. Muller, M. L. denBoer, and S. Horn, Physica B (Amsterdam) **194**, 1217 (1994).
[21] F. M. F. deGroot, M. Grioni, J. C. Fuggle, J. Ghijsen, G. A. Sawatzky, and H. Petersen, Phys. Rev. B **40**, 5715 (1989).
[22] A. Zylbersztejn and N. F. Mott, Phys. Rev. B **11**, 4383 (1975).
[23] S. Biermann, A. Poteryaev, A. I. Lichtenstein, and A. Georges, Phys. Rev. Lett. **94**, 026404 (2005).